2008 American Control Conference
Westin Seattle Hotel, Seattle, Washington, USA
June 11-13, 2008

Stabilization of a 2-DOF Inverted Pendulum by a Low Cost Visual Feedback

Haoping Wang, Afzal Chamroo, Christian Vasseur and Vladan Koncar

Abstract—**This paper presents a stabilization control system of a 2-DOF inverted pendulum. The challenge is to realize a control with a contact-less feedback including a low cost CCD camera. The global control system uses two feedback loops. The first one (inner loop) includes the delayed and sampled inverted pendulum's top coordinates, obtained from the CCD camera and the second one (outer loop) concerns the cart's position in continuous time (obtained from encoders). With this feedback scheme, we propose a specific control method by choosing an optimal balancing plane at each camera's sampling instant, in view of transforming the 2-DOF pendulum problem to a 1-DOF one. Then in this balancing plane, we realize two control loops: The inner loop, relative to the pendulum's angle, is controlled by a linearization and stabilization method based on an innovative observer called Piecewise Continuous Reduced-Order Luenberger Observer (PCROLO). The outer loop uses a Lyapunov function based control scheme with slower internal dynamics compared to that of the pendulum, considering that the global controlled system (cart + pendulum) is an unstable non-minimum-phase system. Numerical simulations show that the stabilization control of the inverted pendulum on an x-y robot that are strongly non linear is successful.**

I. Introduction

The inverted pendulum system is a perfect benchmark for the design of a wide range of nonlinear control theories because of it's inherent instability with highly non-linear dynamics. The most considered inverted pendulums are: single, double or triple inverted pendulum on a cart [2], [4], [7], [9], [15], [18], [22], a rotational single-arm or two-link pendulum [20] and an inverted pendulum on an x-y robot [13], [5], [6], [24]. In almost all cases, controllers use continuous accurate sensors which are in physical contact with the pendulum.

However, in numerous applications it is impossible to put sensors in direct contact with the controlled object. Vision systems are a means to avoid this physical constraint. Moreover, from an economical point of view it may be interesting to develop robust control methods that do not require high accuracy and expensive sensors.

Therefore, our challenge is to consider low cost CCD cameras as contactless pendulum sensor. The problem is that these sensors are less accurate and often deliver sampled and delayed signals due to their digital nature and computation-transfer time (image processing) respectively.

Using visual feedback to control a robot is commonly termed as visual servoing [12]. For example visual (image based) features such as points, lines and regions can be used to enable the alignment of a manipulator/gripping mechanism with an object. Hence, vision is a part of a control system providing feedback. However, traditionally visual sensing and manipulation are combined in an open-loop configuration, 'looking' and 'moving' [20], or just for visualizations and animations [1]. Recently, visual supervision has been gradually combined in the closed control loop particularly for cart-inverted pendulum control such as in [8], [23]. Unfortunately there is no real successful application reported on controlling the pendulum and the cart's position by visual servoing till now. Only a fuzzy-logic based controller was reported in [16], but just for controlling the pendulum. The PID+Q controller has been applied to antisway control of crane lifter modeled by the structure of an inverted pendulum [17]. Unfortunately, there is no research work related to an inverted pendulum on an x-y robot using visual feedback has been reported.

Analyzing difficulties of previous vision based research works related to inverted pendulum control; it seemed that the camera signal has not been sufficiently exploited. Therefore, our efforts have been focused on the development of the accurate observer using the theory of Piecewise Continuous Systems (PCS) [14] to compensate the delayed, imprecise sampled data of the vision system. The improved signal is generated in continuous time.

The research results presented here are an extension and development of the previous works [14], [3], [21], especially relative to the use of the PCS in order to design a PCROLO that compensates the time delay and the sampling effects introduced by the visual feedback.

In this article, the control scheme implemented via a cascade combination method is inspired by the work of K. Guemghar et al. [10]. The control method based on a PCROLO and linearization and stabilization control applied to control the pendulum's angle form the inner loop. In parallel, a Lyapunov based control for the unstable non-minimum-phase internal system (cart) with slower dynamics

This work was supported by the Nord - Pas de Calais region, the France state and the European Community with the contract 15010/02Y0064/03-04 CAR/Presage N° 4605 Obi. 2-2004:2 - 4.1 - N° 160/4605. The authors would like to thank them for their kind support.

H.P. Wang, C. Vasseur, are with LAGIS CNRS UMR 8146, Université des Sciences et Technologies de Lille, UFR IEEA, Bâtiment P2 – 314/204, 59655 Villeneuve d'Ascq Cedex, France (e-mail: (haoping.wang@ed.univ-lille1.fr, and (Christian.vasseur@univ-lille1.fr).

A. Chamroo is with Université de Poitiers, LAII, 40 avenue du recteur Pineau, 86022 Poitiers, France (e-mail: afzal.chamroo@univ-poitiers.fr).

And V. Koncar is with GEMTEX/ENSAIT 9 rue de l'Ermitage, BP 30329, 59056 Roubaix, France (e-mail: vladan.koncar@ensait.fr).

comparing to the pendulum dynamics constitutes the outer loop. Simulation results are given at the end of the paper.

II. Experimental Platform

The vision based control platform of the 3D inverted pendulum presented in Fig. 1 contains the next four parts:

A. The Mechanical X-Y table (Fig. 1)

The system is composed of an X-Y aluminum chassis and a plastic inverted pendulum mounted on the mobile cart. Between the pendulum and the cart, a circular shock absorber preventing the pendulum from completely falling to horizontal position is installed. It allows the pendulum to have a maximum angle of ±50° with respect to the vertical position.

Axes are actuated by AC servo motors via notched belt.

B. Vision system

Instead of using hi-tech digital cameras capable of higher sampling rates, higher spatial resolution and improved signal/noise ratio, we used a low cost IR CCD (Jai M50 IR) camera with a sampling rate of 25 frames/sec and a low resolution of 640 × 480 pixels in non-interlaced mode. The measurements of the camera are available at a sampling rate of T = 40 ms (acquisition-processing-transferring time). In order to simplify the data sensing, an infrared LED has been added on the upper tip of pendulum.

The vision computer is equipped with an image acquisition card (ELTEC PC-EYE 4). Image processing is realized by software called TEKVIS that detects the inverted pendulum's upper tip (x, y) coordinates and transmits them to the control computer via the RS-232 serial communication. In order to synchronize the camera with the controller, the camera is triggered by an external periodical pulse signal, generated via the dSpace card with a sampling period equal the acquisition-processing-transferring time.

As soon as the control computer receives the pendulum's coordinates, a four step "TSAI" calibration method [11] is carried out. It supports not only the real inverted pendulum top position but also the compensation of the deformations caused by the camera's lenses. Moreover, the difference in the height of the pendulum's upper tip plays an important role in the projective imaging geometry of the camera. Hence, two points with a same coordinate in x-y plane but in different height project to two different points in the image, affecting the sensing results and accuracy.

C. The controller

The controller is implemented on a dSpace DS1103 card on a control computer. The ControlDesk module integrated with Matlab/Simulink, enables the modeling, the supervision and the development of direct control methods for the real system using control card's variables and parameters. The control signals are sent to power amplifiers via ± 10 V DAC.

D. The actuators

This part of the system is composed of two servo motors (SANYO DENKI PY2A015A3-A3), whose configurations can be modified and parameterized via the RS-232 serial communication by the PY software in the control computer. AC motors P50B050020DXS00M, driven by a dSpace computer input/output card via a power amplifier, are actually mounted on each axis of the X-Y table. The amplifier is supplied with 240 V. The AC motors deliver a nominal couple of 3.0 Nm with a power of 200 W. The platform provides the cart's x, y position through encoders.

III. Modeling the Inverted Pendulum System

In [13], [5], [6], [24], the authors propose an approximately decoupled modeling method for a 2-DOF inverted pendulum with the constraint of working in a small angle inclination. As compared to this method, we propose here a different modeling approach without any restriction. Its main idea consists in choosing an optimal plane in view of transforming a 2-DOF inverted pendulum problem in a 1-DOF problem.

A. Inverted Pendulum (cf. Fig. 2)

Initially, we consider the $Px'y'z'$ reference parallel to the $Oxyz$ reference of the cart-pendulum system, with point P being the pivot of the pendulum. At any time, the inverted pendulum can be projected onto two orthogonal planes: r-z' (including the entire inverted pendulum) and x-y plane (parallel to two directions of the X-Y table), as illustrated in Fig.2. According to the main modeling idea, the r-z' plane has been chosen as the optimal one to balance the pendulum. Therefore, the 2-DOF problem is reduced to a 1-DOF one.

By referring to the methods proposed in [2], [7], the 2-DOF inverted pendulum can be modeled as follows

$$\ddot{\theta} + 2\zeta\omega_n\dot{\theta} - {\omega_n}^2 \sin\theta = -K\cos\theta\ddot{r} \tag{1}$$

where: $\omega_n = \sqrt{mgl/(J+ml^2)}$ natural frequency ,

$\zeta = B_r/[2\omega_n(J+ml^2)]$ damping ratio,

$K = ml/(J+ml^2)$ the gain,

with: θ the angle of the pendulum with z-axis in the r-z' plane, l the length from the pendulum's center of gravity to the pivot, m the mass of the pendulum, B_r the viscous damping constant between the pendulum and the cart, g the gravitational acceleration, $J=(ml^2)/3$ the pendulum momentum of inertia and r the cart's position on r-axis, considering the origin of this axis to be O' which is the orthogonal projection of O on r-axis. Naturally, the displacement on r-axis is the result of a combination on x and y axes.

Moreover, by considering the projection of the pendulum on the x-y plane, as shown in Fig. 3, we can find the geometrical relationship between x, y and r:

$$r = x\cos\alpha + y\sin\alpha \quad (2)$$

with α the angle between r and x axes and calculated by (5).

B. Motor-Cart System

On x-axis, the motor-cart model which considers the motor terminal voltage u_x as its input and the motor's horizontal displacement x as its output, can be modeled as follows

$$\ddot{x} = (-\dot{x} + k_x u_x)/\tau_x \quad (3)$$

where: k_x the overall gain of the motor-cart on x-axis,
τ_x the time constant of the motor-cart on x-axis.

In the same way, the motor-cart on y-axis is modeled as

$$\ddot{y} = (-\dot{y} + k_y u_y)/\tau_y . \quad (4)$$

C. Pendulum's Angles Computation (α and θ)

According the structure of our platform, the only accessible information are the coordinates (x_C, y_C) of the pendulum's upper tip projection on the x-y plane via the vision system and the pendulum's pivot coordinates (x, y) via x and y encoders.

In these conditions, according to Fig. 2 and Fig. 3, the α and θ angles can be computed as follows

$$\alpha = \tan^{-1}\left[(y_C - y)/(x_C - x)\right], \quad (5)$$

$$\theta = \sin^{-1}\left\{\left[(x_c - x)\cos\alpha + (y_c - y)\sin\alpha\right]/2l\right\}. \quad (6)$$

In our case, only sampled and delayed measurements of the camera are available

$$(x_C(kt_e - T_e), y_C(kt_e - T_e)) = (x_{C,k-q}, y_{C,k-q}) \quad (7)$$

with t_e the camera's sampling cycle, and $T_e = qt_e$. where: q is an integer number and T_e represents the delay time corresponding the time necessary for data acquisition, processing and transfer. For our vision system, t_e=40 ms and q=1.

Finally, from (5), (6) and (7), α_{k-1} and θ_{k-1} are computed.

IV. Inverted Pendulum Control

The main control architecture for the 2-DOF pendulum is presented in Fig. 4. The hybrid feedback generates the continuous cart coordinates (x, y) and the delayed and sampled pendulum's angular position θ_{k-1}. The control principle is that at each sampling instant an optimal balancing plane r-z' is selected by using α_{k-1}. Then, in this balancing plane, the control system is built considering two loops. The first one (inner loop) realizes a linearization and the stabilization control of the pendulum based on the innovative observer of PCROLO coupled with a linearization module. The second one (the outer loop) realizes a Lyapunov based control for the unstable internal system having slower dynamics than that of the pendulum.

The aim is to find two controls u_x and u_y by introducing an intermediate pendulum's reference angle θ_{ref} which ensures the global stability of the 2-DOF cart-pendulum system.

A. Stabilization of the Inverted Pendulum

Under the assumption that the inverted pendulum's angular position θ and velocity $\dot{\theta}$ are precisely estimated via the PCROLO, the 1-DOF inverted pendulum's dynamic equations in (1) lead to

$$\ddot{r} = \tilde{v}, \quad (8)$$

$$\ddot{\theta} + 2\zeta\omega_n\dot{\theta} - \omega_n{}^2\sin\theta = -K\cos\theta\tilde{v}. \quad (9)$$

In order to stabilize the pendulum, a stable dynamics can be imposed by introducing a new control v, a new gain K_2, a new natural frequency Ω_n and a new damping ratio Z defined as follows

$$-2\zeta\omega_n\dot{\theta} + \omega_n{}^2\sin\theta - K\cos\theta\tilde{v} = -2Z\Omega_n\dot{\theta} - \Omega_n^2\theta + K_2 v. \quad (10)$$

From (10) the relation between $\tilde{v}$ and v is

$$\tilde{v} = \left[-2(\zeta\omega_n - Z\Omega_n)\dot{\theta} + \Omega_n^2\theta + \omega_n{}^2\sin\theta - K_2 v\right]/K\cos\theta \quad (11)$$

with: $|\theta| < \pi/2$. After the transformation, one has

$$\ddot{r} = \left[-2(\zeta\omega_n - Z\Omega_n)\dot{\theta} + \Omega_n^2\theta + \omega_n{}^2\sin\theta - K_2 v\right]/K\cos\theta, \quad (12)$$

$$\ddot{\theta} + 2Z\Omega_n\dot{\theta} + \Omega_n^2\theta = K_2 v. \quad (13)$$

Thus, from (13), the linearized pendulum's state equation is

$$\dot{\Theta}(t) = A\Theta(t) + Bv(t) \quad (14)$$

with $A = \begin{bmatrix} 0 & 1 \\ -\Omega_n^2 & -2Z\Omega_n \end{bmatrix}$, $B = \begin{bmatrix} 0 \\ K_2 \end{bmatrix}$ and $\Theta(t) = \begin{bmatrix} \theta(t) \\ \dot{\theta}(t) \end{bmatrix}$.

B. PCROL Observer

The problem is to estimate the continuous position θ and velocity $\dot{\theta}$ from the visual feedback θ_{k-1}. In order to resolve this problem, a specific PCROLO is designed. This observer combines a Reduced-Order Discrete Luenberger Observer (RODLO) and two Piecewise Continuous Systems (PCS) as defined in [12]. A PCS $\Sigma(\{kt_e\}, A, B, C)$ is symbolized by Fig. 5. It is characterized by a first continuous input $\varphi(t)$, a second input $\psi(t)$ sampled at discrete instants kt_e, three state matrices A, B and C, a state vector $x(t)$ and an output vector $y(t)$. In these conditions, the functioning equations are as follows

$$x_k(t) = \exp(A(t-kt_e))\psi(kt_e) + \int_{kt_e}^{t} \exp A(t-\tau)B\varphi(\tau)d\tau,$$
$$y_k(t) = Cx_k(t),\ \forall t \in [kt_e, (k+1)t_e[\ . \quad (15)$$

In order to observe $\Theta(t)$, we choose A and B as in (14) and $C=I_2$.

According to Fig. 6, the PCROLO is constructed as follows:

First step: PCS I

Using the PCS I, with φ(t)=$v(t)$ and $\psi(t)$=0, one has

$$M_{k-1}(t) = \int_{(k-1)t_e}^{t} \exp A(t-\tau)Bv(\tau)d\tau.$$

By sampling (ZOH) at each kt_e, one obtains

$$M_{k-1}^{k} = \int_{(k-1)t_e}^{kt_e} \exp A(kt_e-\tau)Bv(\tau)d\tau = \begin{bmatrix} m1_{k-1}^{k} \\ m2_{k-1}^{k} \end{bmatrix}.$$

Second step:RODLO

Θ_{k-1} is estimated by a RODLO defined below

$$z_k = Fz_{k-1} + G\theta_{k-1} + (m2_{k-1}^{k} - Lm1_{k-1}^{k}),$$
$$z_{k-1} = \dot{\hat{\theta}}_{k-1} - L\theta_{k-1},$$

where F, G and L are defined from as follows:

$\exp(At_e) = \begin{bmatrix} f_{11} & f_{12} \\ f_{21} & f_{22} \end{bmatrix}$, $F = (f_{22} - Lf_{12})$,

$G = (f_{22} - Lf_{12})L + (f_{21} - Lf_{11})$, $L = (f_{22}/f_{12}) \in R$

(imposed value to maximize the RODL Observer's convergence speed).

Estimating $\dot{\theta}_{k-1}$ by $\dot{\hat{\theta}}_{k-1} = z_{k-1} + L\theta_{k-1}$, one gets $\hat{\Theta}_{k-1}$, then $\hat{\Theta}_k$, by integration of (14) on the time interval $[(k-1)t_e, kt_e[$

$$\hat{\Theta}_k = \exp(At_e)\hat{\Theta}_{k-1} + M_{k-1}^{k}.$$

Third step: PCS II

Using the PCS II, with φ(t)=$v(t)$ and $\psi(t) = \hat{\Theta}_k$, one has

$$\hat{\Theta}(t) = \exp(At)\hat{\Theta}_k + \int_{kt_e}^{t} \exp A(t-\tau)Bv(\tau)d\tau. \quad (16)$$

C. Lyapunov Function Based Cascade Control

The main idea of the control scheme is to introduce an angular reference θ_{ref} as an intermediate for the pendulum angular position in the aim of finding the two controls (u_x, u_y).

Applying the quasi-steady state assumption in (12) and (13), the inverted pendulum system is brought to $\ddot{\theta} = \dot{\theta} = 0$, and $\theta=\theta_{ref}$. Thus the simplified dynamic system becomes

$$\ddot{r} = \tilde{v} = [\omega_n{}^2 \tan(\theta_{ref})]/K, \quad (17)$$
$$v = (\Omega_n^2\theta_{ref})/K_2. \quad (18)$$

Based on this internal 2-DOF pendulum system, a Lyapunov candidate function is defined as follows

$$V(r,\dot{r}) = (\chi r^2 + \delta\dot{r}^2)/2, \text{ with } \chi, \delta \geq 0.$$

In order to ensure the Lyapunov derivation's negativity

$$\dot{V}(r,\dot{r}) = \dot{r}(\chi r + \delta\ddot{r}) = \dot{r}(\chi r + \delta\tilde{v}) < 0,$$

a particular function which stabilizes its internal dynamics is selected

$$(\chi r + \delta\tilde{v}) = -\mu[1 - e^{-(\chi r^2 + \delta\dot{r}^2)/2}]\dot{r}, \quad \mu > 0.$$

Therefore, we have

$$\tilde{v} = -[\chi r + \mu(1 - e^{-(\chi r^2 + \delta\dot{r}^2)/2})\dot{r}]/\delta \quad (19)$$

and then replacing (19) in (17), the intermediate value θ_{ref} can be computed. Then, by substituting θ_{ref} in (18), the control v is given

$$v = f_1(r,\dot{r}) = (\Omega_n^2\tilde{f}_1)/K_2 \quad (20)$$

with $\tilde{f}_1 = \tan^{-1}\left\{-K[\chi r + \mu(1 - e^{-(\chi r^2 + \delta\dot{r}^2)/2})\dot{r}]/(\delta\omega_n{}^2)\right\}$.

The last step is to find the relations between the control $\tilde{v}$ and the two controls u_x and u_y as illustrated in Fig 4.

Considering (2) (3) and (4) with local input/output injection for each motor, we can obtain: $k_x=k_y=k$ and $\tau_x=\tau_y=\tau$. In these conditions, the balancing of the pendulum in the r-z' plane is ensured by imposing the following additional condition for the cart's accelerations $\ddot{y}/\ddot{x} = \tan\alpha$.

Finally u_x and u_y are defined as follows

$$u_x = (\dot{x} + \cos\alpha\tau\tilde{v})/k, \quad (21)$$
$$u_y = (\dot{y} + \sin\alpha\tau\tilde{v})/k. \quad (22)$$

V. Numerical Simulations

The mass of the pendulum is 38 g and its length is 31.5 cm, the viscous friction between the pendulum and the cart on the x-y robot is supposed zero. Therefore, according to the modeling procedure, the inverted pendulum is characterized by $\zeta = 0.002$ and $\omega_n = 6.781$. Moreover,

$k = 2.92$ and $\tau = 0.008$ have been chosen. For the controller part, $K_2 = \omega_n^2$, $\xi = 1.2$, $\Omega_n = \omega_n$, $\chi = 1$, $\delta = 2$ and $\mu = 0.5$ by taking into account the performance and stability.

A. Simulation Results

As indicated in Fig. 7, an initial conditions for $\{\alpha, \theta, x, y\}$ as $\{\alpha_0 = \pi/3$ rad, $\theta_0 = \pi/6$ rad, $x_0 = 1$ m and $y_0 = 0.2$ m$\}$ are adopted to validate our method. Figures include: (a) balancing plane projected in x-y plane, (b) x, y and r displacements, (c) pendulum's angles (θ_{k-1}, θ, $\hat{\theta}$) (d) pendulum's angular velocities ($\dot{\theta}$, $\dot{\hat{\theta}}$) and finally (e) controls (u_x, u_y).

The proposed two loops control leads to the stabilization of the entire cart-pendulum system. Note that the cart is stabilized around *O'* (projection of *O* on the balancing plane and origin of r axis). The results illustrate the theoretical aspects of our method, showing precision and reactivity of the PCROLO. Moreover, it shows that the use of the Lyapunov function used in the outer loop assures the whole system's larger convergence stability compare to the standard PID or linearization feedback controls.

B. Robustness consideration

In the real vision system, there always exists a not ignoring measuring error, especially when we use a low-cost camera (40 ms). In order to demonstrate the effective and robustness of the method, we add the same perturbations $0.03\sin(2\pi t)$ and white noise [0.0001] to the measurements $\{\theta_{k-1}, \alpha_{k-1}\}$. The simulation results are given in Fig. 8 under the same initial condition like Fig.7.

VI. Conclusion And Perspectives

The numerical simulations demonstrated the effectiveness and robustness of our method for a class of underactuated non linear system with a non-minimum internal dynamics even with a big measuring error of the vision based system.

The assumptions made for the vision system mainly depending on the real successful application of a low-cost vision based Cart-inverted pendulum control under a big initial condition. Illustrative videos are available on http://www-lagis.univ-lille1.fr/~wang/Research_eng.html.

References

[1] A.R. Armando, P.M. Richard, C. Oguzhan and D. Thanate, "Description of a modelling, simulation, animation, and real-tile control (MoSART) environment for a class of electromechanical systems ," *IEEE Trans. on Education*, Vol. 48, No. 3, pp. 359-374, Aug. 2005.

[2] M. Bugeja, "Non-linear swing-up and stabilizing control of an inverted pendulum system," *EUROCON*, Ljubljana, Slovenia, 2003.

[3] A. Chamroo, C. Vasseur, and H.P. Wang, "Plant control using digital sensors that introduce a delayed and sampled output," *11th ELMA World Congress* , Vol. 1, pp. 119-124, Sofia, Bulgaria, Sep. 2005.

[4] L. Chen and R. Smith, "Closed-loop model validation for an inverted pendulum experiment via a linear matrix inequality approach," *Proc. Of the 36th CDC*, pp. 2565-2566, San Diego, USA, Dec 1997.

[5] Hyun Taek Cho and Seul Jung, "Balancing and Position Tracking Control of an Inverted Pendulum on an X-Y Plane Using Decentralized Neural Networks," *Proc. of 2003 IEEE/ASME Inter. Conf. on Advanced Intelligent Mechatronics*, pp. 1210-1215, 2003.

[6] Hyun-Taek Cho and Seul Jung, "Neural Network Position Tracking Control of an Inverted Pendulum by an X-Y Table Robot" *Proc. of the 2003 IEEB/RSJ Int. Conf. on Intelligent Robots and Systems*, pp. 181-186, Las Vegas, Oct 2003.

[7] D. W. Deley, "Controlling an inverted pendulum: example of a digital feedback control system," Jan 4, 2007, Available: http://members.cox.net/srice1/pendulum/index.htm.

[8] E.S. Espinoza-Quesada and L.E. Ramos-Velasco, "Vision based control of an underactuated system using a reduced observer," *Electronics, Robotics and Automotive Mechanics Conference,* Vol. 1, pp. 9-14, Sep. 2006.

[9] R. Fierro, F.L. Lewis and A. Lowe, "Hybrid control for a class of underactuated mechanical systems," *IEEE Trans. on Systems, Man, and Cybernetics-Part A: Systems and Humans*, Vol. 29, No. 6, pp. 649-654, 1999.

[10] K. Guemghar, B. Srinivasan, Ph. Mullhaupt and D. Bonvin, "Analysis of cascade structure with predictive control and feedback linearization," *IEE Control Theory & Applications*, Vol. 152, No. 3, pp. 317-324, May 2005.

[11] J. Heikkila and O. Silven, "A four-step camera calibration procedure with implicit image correction," *1997 IEEE Computer Society Conference on Computer Vision and Pattern Recognition*, pp.1106-1112, Jun 1997.

[12] S. Hutchinson, G.D. Hager and P.I. Corke, "A tutorial on visual servo control," *IEEE Trans. on Robotics and Automation*, Vol. 12, No. 5, pp. 651-670, Oct. 1996.

[13] S. Jung and H.T. Cho, "Decoupled neural network reference compensation technique for a PD controlled two degrees-of-freedom inverted pendulum," *Int. J. of Control, Automation and Systems*, Vol. 2, No. 1, pp. 92-99, March 2004.

[14] V. Koncar and C. Vasseur, "Control of linear systems using piecewise continuous systems," *IEE Control Theory & Applications*, Vol. 150, n° 6, pp. 565-576, Nov. 2003.

[15] R. Lozano, I. Fantoni and D. J. Block, "Stabilization of the inverted pendulum around its homoclinic orbit," *Systems & Control Letters*, Vol. 40, pp. 194-204, 2000.

[16] M.E. Magana and F. Holzapfel, "Fuzzy-logic control of an inverted pendulum with vision feedback," *IEEE Trans. On Education*, Vol. 41, Issue 2, pp. 165-170, May 1998.

[17] T. Matsuo, R. Yoshino, H. Suemitsu and K. Nakano, "Nominal performance recovery by PID+Q controller and its application to antisway control of crane lifter with visual feedback," *IEEE Trans. on Control System Technology*, Vol. 12, No.1, pp. 156-166, Jan. 2004.

[18] A. Ohsumi and T. Izumikawa, "Nonlinear control of swing-up and stabilization of an inverted pendulum," *Proc. Of the 34th CDC*, New Orleans, pp. 3873-3880, Dec. 1995.

[19] R. Olfati-Saber, "Fixed point controllers and stabilization of the cart-pole system and the rotating pendulum," *Proc. Of the 38th CDC*, Phoenix, pp. 1174-1181, Dec 1999.

[20] J. Sanchez, S. Dormido R. Pastor and F. Morilla, "A Java/Matlab-based environment for remote control system laboratories: illustrated with an inverted pendulum," *IEEE Trans. on Education*, Vol. 47, No. 3, pp. 321-329, Aug. 2004

[21] H. P. Wang, C. Vasseur, A. Chamroo and V. Koncar, "Sampled tracking for delayed systems using piecewise functioning controller," *4th IEEE conf. on Computational Engineering in Systems Applications*, Vol. 2, Beijing, China, Oct. 2006.

[22] Q. Wei, W.P. Dayawansa and W.S. Levine, "Nonlinear controller for an inverted pendulum having restricted travel," *Automatica*, Vol. 31, No. 6, pp. 841-850, 1995.

[23] L. Wenzel, N. Vazquez, D. Nair and R. Jamal, "Computer vision based inverted pendulum," Proc. of the 17th IEEE Instrumentation and Measurement Technology Conference. Vol. 3, pp.1319-1323, may 2000.

[24] R. Yang, Y. Kuen and Z. Li, "Stabilization of A 2-DOF Spherical Pendulum on X-Y Table," *Proc. Of the 2000 IEEE International Conference on Control Applications*, pp. 724-729, USA, Sep 2000.

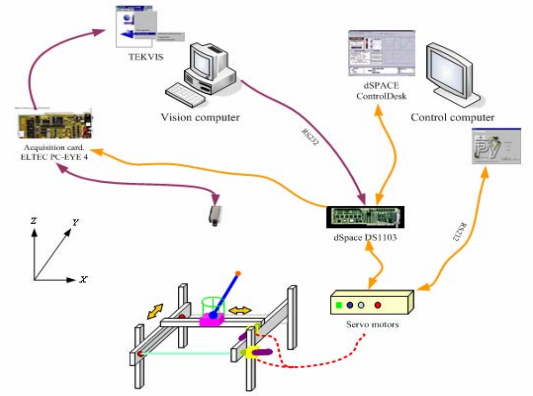

Fig. 1. Experimental platform.

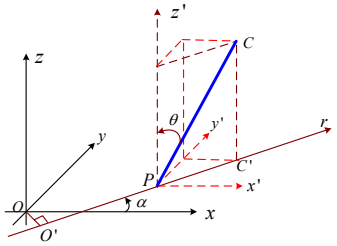

Fig. 2. Inverted pendulum on the r-z and x-y-z planes

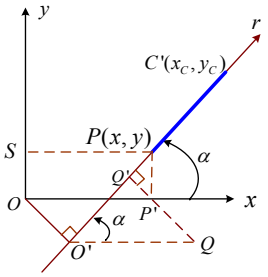

Fig. 3. Projection of inverted pendulum on the x-y plane

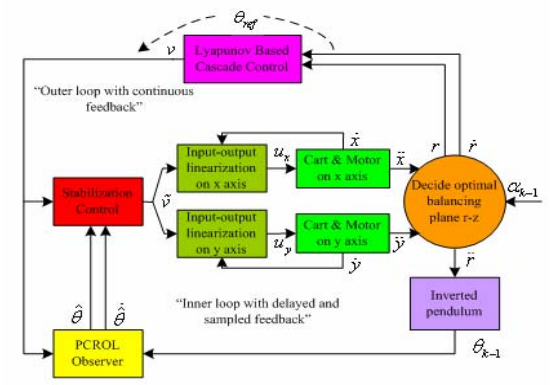

Fig. 4. The 2-DOF Inverted pendulum control architecture

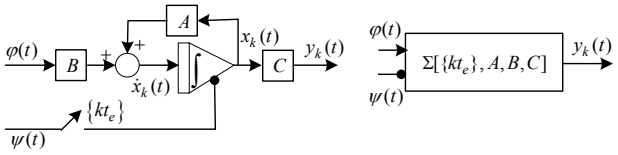

Fig. 5. a) PCS detailed structure b) PCS symbolic representation

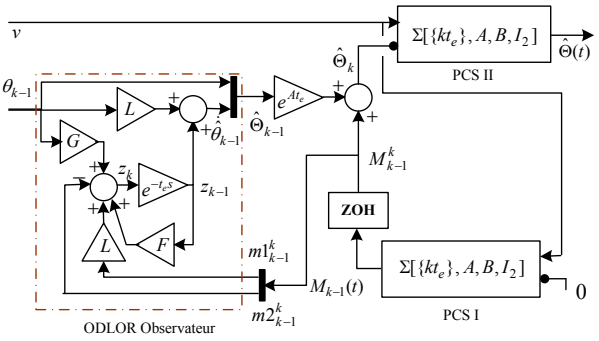

Fig. 6. Piecewise Continuous Reduced Order Luenberger Observer

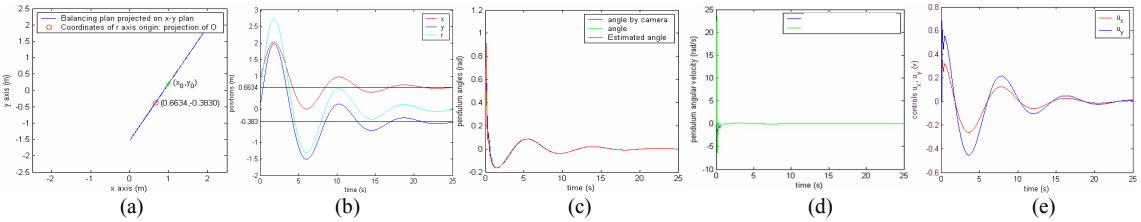

(a) (b) (c) (d) (e)

Fig. 7. Simulation result: $\{\alpha_0 = \pi/3$ rad, $\theta_0 = \pi/6$ rad, $x_0 = 1$ m and $y_0 = 0.2$ m$\}$

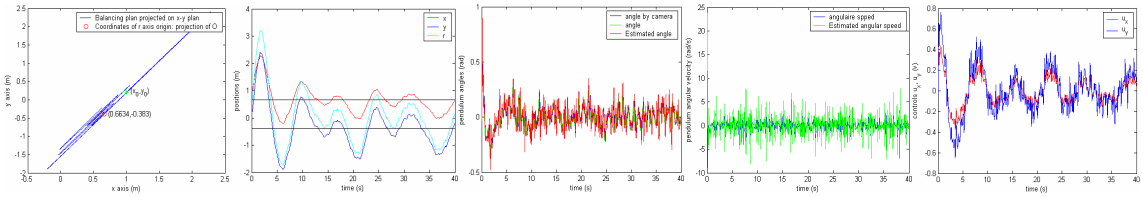

(a) (b) (c) (d) (e)

Fig. 8. Simulation result under measuring error and white noise $\{\alpha_0 = \pi/3$ rad, $\theta_0 = \pi/6$ rad, $x_0 = 1$ m and $y_0 = 0.2$ m$\}$